ELSEVIER

Guanosine and fullerene derived de-aggregation of a new phthalocyanine-linked cytidine derivative

Jonathan L. Sessler,[a,*] Janarthanan Jayawickramarajah,[a] Andreas Gouloumis,[b] G. Dan Pantos,[a] Tomás Torres[b,*] and Dirk M. Guldi[c,*]

[a]Department of Chemistry and Biochemistry and Institute for Cellular and Molecular Biology, 1 University Station, A5300, University of Texas at Austin, Austin, TX 78712-0165, USA
[b]Universidad Autónoma de Madrid, Departmento de Química Orgánica, Campus de Cantoblanco, Madrid, Spain
[c]Universität Erlangen, Institute for Physical and Theoretical Chemistry, 91058 Erlangen, Germany

Abstract—Electronic absorption and emission properties of a new cytidine tethered zinc phthalocyanine **2** were used to probe the aggregation and guanosine/C_{60} derived de-aggregation of this nucleobase linked phthalocyanine. These experiments revealed that **2** aggregates even at low concentrations in a competitive solvent system (1.1×10^{-6} M in 20% DCM/toluene). Nucleobase–metal coordination and slipped co-facial π-stacking interactions are both important in aggregate formation. Guanosine **5**, C_{60} **6**, and a guanosine-C_{60} chimera **4** were employed as potential aggregate disruptors. These experiments revealed that both guanosine and fullerene subunits are effective in disrupting the aggregate formed by **2**. Such findings support the conclusion that base-pairing, π-stacking, as well as nucleobase–metal coordination interactions play important roles in the de-aggregation of **2**.
© 2005 Elsevier Ltd. All rights reserved.

1. Introduction

Phthalocyanines (Pcs), and their metallated congeners, are an important class of non-natural organic pigments that have received considerable attention in recent years.[1] These 18 π-electron macrocyclic systems have shown considerable promise for a wide range of applications, including as materials for optical data storage[2] and nonlinear optics,[3] as well as photosensitizers for photodynamic therapy.[4] The common denominator in these applications is the useful photophysical properties of Pcs. In fact, these highly colored molecules absorb intensely in the 700 nm spectral range, a region where the solar photon flux is a maximum. Furthermore, once illuminated Pcs are capable of efficient electron donation to fullerene acceptors.[5] These attributes render Pcs especially attractive as possible components in photovoltaic devices that can harvest and convert solar energy into chemical energy.

The propensity of Pcs to self-aggregate through coplanar association of the Pc rings to form dimers and higher order aggregates is well known.[6] This tendency, can cause Pcs to be insoluble in many solvents and can also dramatically affect their photochemical properties. For instance, aggregation has been shown to cause a decrease in light absorption[6,7] and has also been found to induce a large reduction in fluorescence quantum yield.[8] On the other hand, the formation of well-defined Pc aggregates is useful in materials applications where the self-assembly of Pc cores in close proximity is beneficial.[9,2a] In light of such considerations, it is not surprising that methods to manipulate the aggregation/de-aggregation properties of Pcs are being actively pursued.[10]

We and others have focused our efforts on using non-covalent synthesis as a strategy to assemble Pcs in conjunction with efficient electron acceptors such as fullerenes to study photoinduced electron transfer.[11] These systems have been assembled through various non-covalent interactions such as, ligand–metal coordination, π-stacking, and hydrogen bonding interactions. In this paper, we report the use of these non-covalent interactions to effect the aggregation and de-aggregation of a cytidine tethered zinc phthalocyanine (ZnPc) **2**. Specifically, we show how guanosine **5**, C_{60} **6**, and a guanosine–C_{60} hybrid **4** may be used to induce the de-aggregation of ZnPc **2** in solution.

2. Aggregation/de-aggregation of phthalocyanines

In general Pc aggregation is thought to reflect coplanar interactions involving the macrocycle ring.[6] These interactions occur as a result of favorable van der Waals forces, π-stacking interactions, and solvent effects. The aggregation process of Pcs can be easily probed using electronic spectroscopy. Upon formation of higher order complexes, the coupling between the electronic states of individual monomeric Pc units causes significant spectral perturbations. For example, monomeric Pcs exhibit strong absorption bands in the 300 and 700 nm spectral regions, termed the B and Q bands, respectively. The presence of higher order Pc systems can be observed in the Q band region of the electronic absorption spectrum. Typically, Pc aggregation results in a decrease in intensity in the components of the Q band corresponding to the monomeric species, meanwhile a new, broader and blue-shifted band is seen to increase in intensity. This shift to lower wavelengths corresponds to H-type aggregates. Rare cases of Pc aggregation causing red-shifted bands, corresponding to J-type aggregation, have also been observed.

3. Results and discussion

3.1. Aggregation behavior of nucleobase appended zinc phthalocyanines

A recent study by Ng and co-workers demonstrated that phthalocyanine-nucleobase conjugates, such as the adenine derivative **1**, can be prepared.[10f] Additionally, it was found that these phthalocyanine conjugates possess a tendency to aggregate as a result of a variety of interaction modes. These intermolecular interactions include the typical π–π interactions between the macrocycle cores that one would expect for Pcs, as well as possible hydrogen bonding interactions due to the nucleobase unit. Another potential mode of interaction, proposed by the

authors, is through axial coordination of adenine to the zinc(II) center of the phthalocyanine macrocycle. A further advantage of using nucleobase tethered systems is the possibility of forming Watson–Crick base-pairs by the addition of a complementary nucleobase. Accordingly, in the same paper, Ng and colleagues have also investigated the base-pairing capability of adenine substituted Pcs with a thymine derivative.

Inspired by these initial nucleobase linked ZnPc systems, we have prepared cytidine tethered ZnPc **2**. It was rationalized that this novel nucleobase appended ZnPc should form stronger Watson–Crick base-pairing interactions than Pc **1**, because, the cytidine motif can form three-point hydrogen bonding interactions with a guanine moiety, whilst the adenine–thymine base-pair is only stabilized by two hydrogen bonds.[12] Furthermore, in this new system, a rigid alkynyl linker was used to tether the pyrimidine nucleobase to the ZnPc subunit. It was anticipated that increasing the rigidity of the system would lead to the formation of better-defined self-assemblies, as well as supporting stronger Watson–Crick type base-pairing interactions.[13] In order to enhance solubility in organic solvents, lipophilic *tert*-butyl and *tert*-butyldimethylsilyl (TBDMS) groups were incorporated on the ZnPc and cytidine subunits, respectively.

Given that electronic absorption spectroscopy has been extensively used to determine the formation of Pc aggregation,[6] we carried out our initial studies of aggregation effects with ZnPc **2** using this method. A typical spectrum of **2** (3.9×10^{-6} M), in dichloromethane (DCM), is shown in Figure 1. Two major bands are visible at 347 and 679 nm, respectively. These, so-called B and Q absorption bands are considered to originate from ligand-based π–π* transitions.[14] As is clearly evident from an inspection of Figure 1, the Q-band is rather broad with a significant blue-shifted shoulder appearing at ca. 630 nm. This result is consistent

R = TBDMS
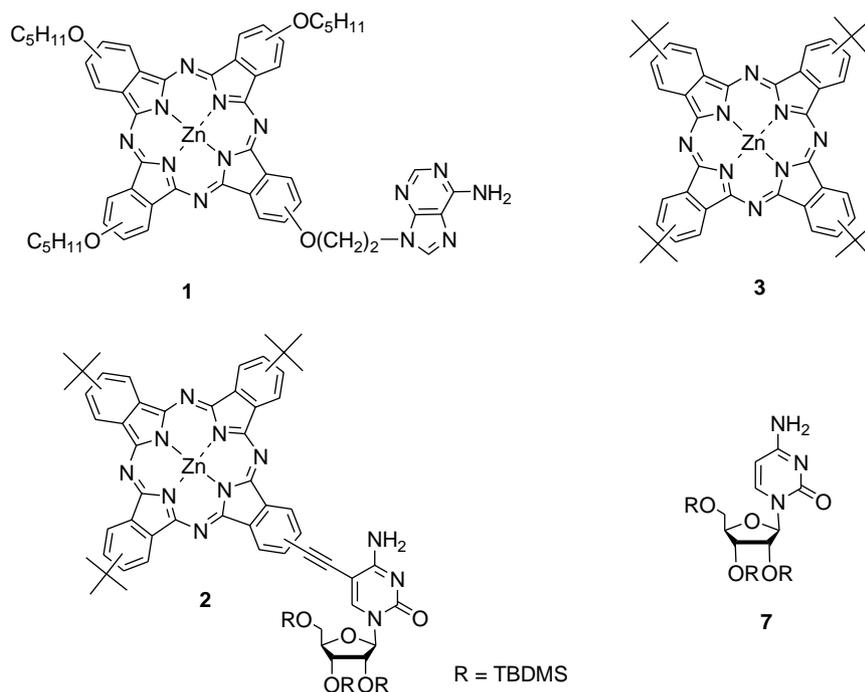
with the conclusion that even at this low concentration regime ZnPc **2** displays significant aggregation behavior. Interestingly, adenine tethered ZnPc **1** at similar concentrations $(6.3 \times 10^{-6} – 1.0 \times 10^{-4}$ M) was found to be free of aggregation in DCM as judged by UV–vis spectroscopy.[10f] Thus, under the conditions of the above experiment, ZnPc **2** has a greater tendency to self-aggregate than the previously reported nucleobase derived ZnPc, system **1**.
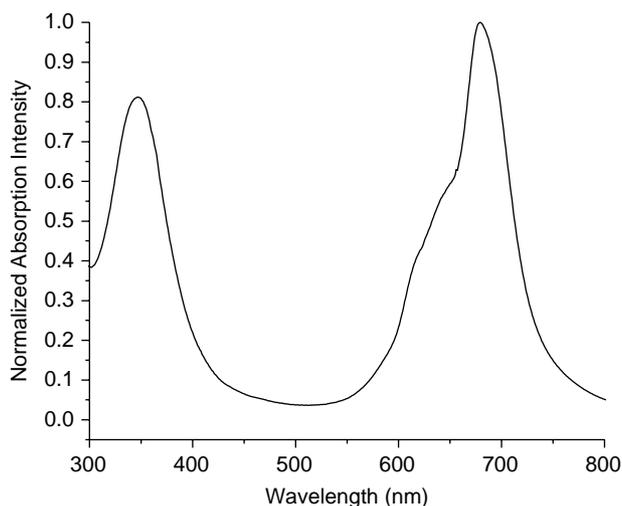

Figure 1. Normalized electronic absorption spectrum of the B- and Q-band regions of ZnPc **2** $(3.9 \times 10^{-6}$ M) in dichloromethane.

UV–vis experiments were also carried out in a more competitive solvent system (20% DCM in toluene), in order to test the stability of the self-aggregate and to elucidate the signature peaks corresponding to the monomeric form of **2**. Toluene was included in the mixture, since it was expected to act as a π–π interaction disruptor. Interestingly, even in this solvent system, at a concentration of 5.7×10^{-5} M, ZcPc **2** is predominantly aggregated (see Fig. 2). Under these conditions, the Q-band region of compound **2** is
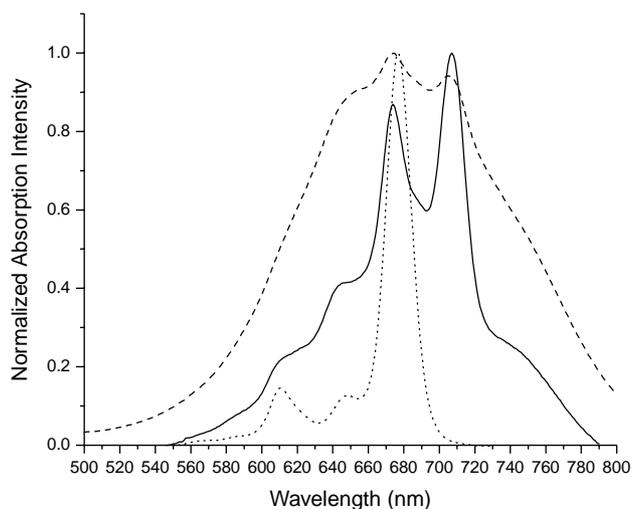

Figure 2. Normalized absorption spectra of the Q-band region of ZnPc **2** (dashed line corresponds to $[\mathbf{2}] = 5.7 \times 10^{-5}$ M, solid line corresponds to $[\mathbf{2}] = 1.1 \times 10^{-6}$ M) and control **3** (dotted line: $[\mathbf{3}] = 2.5 \times 10^{-6}$ M) in 20% DCM/toluene.

characterized by a very broad band, almost void of structure except for one small hump corresponding to a maximum at 674 nm and a second smaller hump at 708 nm. The broadness of the Q-band (the width of which is ca. 127 nm at half height) is considered to be clear evidence of substantial aggregation.

When ZnPc **2** is diluted to a concentration of 1.1×10^{-6} M, evidence of aggregation is still apparent. For instance, the presence of a shoulder at ca. 750 nm is typical of aggregation. However, at this concentration, the absorption features corresponding to the monomeric species are also evident. For instance, a clearly split Q-band, with peaks at 674 and 708 nm, attributed to the monomeric species, is visible.[15] The reason for the split in the Q-band region is thought to reflect the unsymmetric nature of the ZnPc moiety, arising from the introduction of the cytidine motif onto the isoindole ring. Two minor vibrational satellites corresponding to the monomeric species are also observable at ca. 613 and 644 nm. Still, it must be noted that the features present in this region (600–662 nm) are rather broadened, leading us to suggest the underlying presence of a low intensity, blue-shifted absorption band corresponding to one or more aggregated species.

The blue shifting and the broadening in the Q-band region of **2**, ascribed to aggregation are both features that are consistent with linearly stacked Pc monomers.[6] In an effort to understand better the nature of the aggregates formed in the case of **2** and to determine the influence imparted by the cytidine subunit on the overall aggregation process, control studies using tetra-*tert*-butyl ZnPc **3** (lacking the nucleobase functionality) were carried out. As illustrated in Figure 2, ZnPc **3** showed no evidence of aggregation at 2.5×10^{-6} M in 20% DCM/toluene. Rather, an absorption band corresponding only to the monomeric form was observed. In particular, a sharp absorbance maximum at 677 nm (the width of which is ca. 18 nm at half height) was seen, as well as two vibrational satellites at 611 and 648 nm, respectively.

The above mentioned UV–vis experiments indicate that the cytidine subunit and the ZnPc macrocycle are both important in the observed aggregation of **2**. Furthermore, the mode of aggregation results, at least in part, from stacked ZnPc monomers. A proposed mode of aggregation is illustrated in Scheme 1, wherein the aggregate is stabilized by axial coordination of the cytidine subunit to the zinc(II) center that acts in conjunction with slipped cofacial π–π interactions between the Pc macrocycles.

Control studies, involving ZnPc **3** and $2', 3', 5'$-tri-*O-tert*-butyldimethylsilyl protected cytidine **7**, were performed to verify that the cytidine moiety can interact with the ZnPc macrocycle. As cytidine **7** $(0–2.1 \times 10^{-5}$ M) is titrated into a solution containing **3** $(2.5 \times 10^{-6}$ M) in 20% DCM/toluene, a decrease in the absorption maximum at 677 nm is seen. A plot of the change in absorption at 677 nm versus concentration of cytidine **7** displays typical binding behavior (Fig. 3a). Based on these findings, and in analogy to the findings of Ng[10f] and others,[16] it is thought that the cytidine motif interacts with the Pc moiety in **2** through axial coordination to the metal center. Presumably, this occurs through the N3 nitrogen (see Scheme 1), since it is
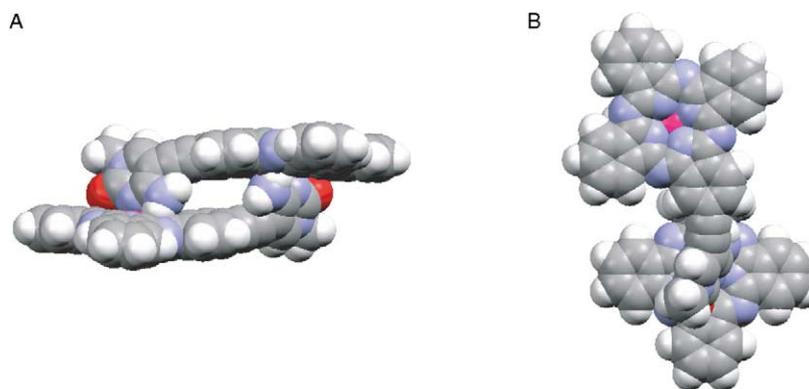
Scheme 1. Computer generated model showing the side view (A) and top view (B) of one possible aggregation mode for ZnPc **2** (for clarity the ribose unit has been replaced by a methyl group and the *t*-butyl motifs have been omitted).

the most basic nitrogen center present on the nucleobase. Further evidence supporting the notion that axial metal coordination may play an important role in the aggregation of ZnPc **2** came from the addition of pyridine into a solution of **2** in 20% DCM/toluene (Fig. 3b). Pyridine is an effective axial ligand for Zn(II) centers constrained within a macrocyclic framework,[18a] and not surprisingly complete disruption of aggregation is seen, as evidenced by the clean monomer-type spectrum.

to complement the functionalities present on ZnPc **2**. For instance, it was envisaged that the guanosine motif on **4** would base-pair with the cytidine subunit of **2**, thus inducing a break up of the self-aggregation normally caused by this subunit. Similarly, the fullerene motif was included since it is known that fullerenes can bind porphyrinoid macrocycles through π–π interactions, and more specifically, that Pcs can interact with fullerenes in solution and in the solid state.[18,5c] In particular, it was thought that the fullerene
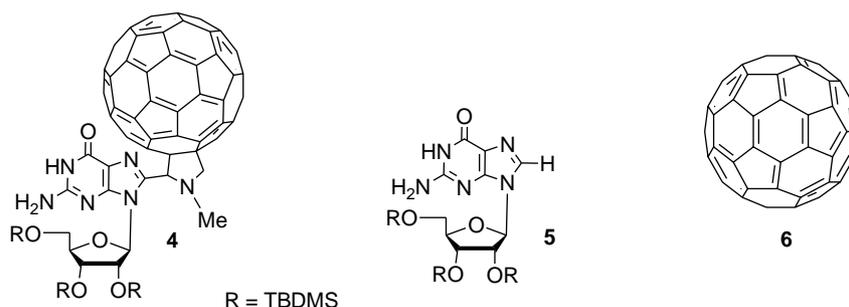
3.2. Disruption of aggregation using guanosine-appended fulleropyrrolidine (4)

In order to promote the disassembly of ZnPc **2**, guanosine derivative **4** was synthesized.[17] This molecule was designed

subunit would induce break up of the aggregate by participating in non-covalent π–π interactions involving ZnPc **2**. Nucleobase **5** and commercially available C_{60} **6** were used as controls to gage the effectiveness of each subunit separately in terms of effecting aggregate breakup.
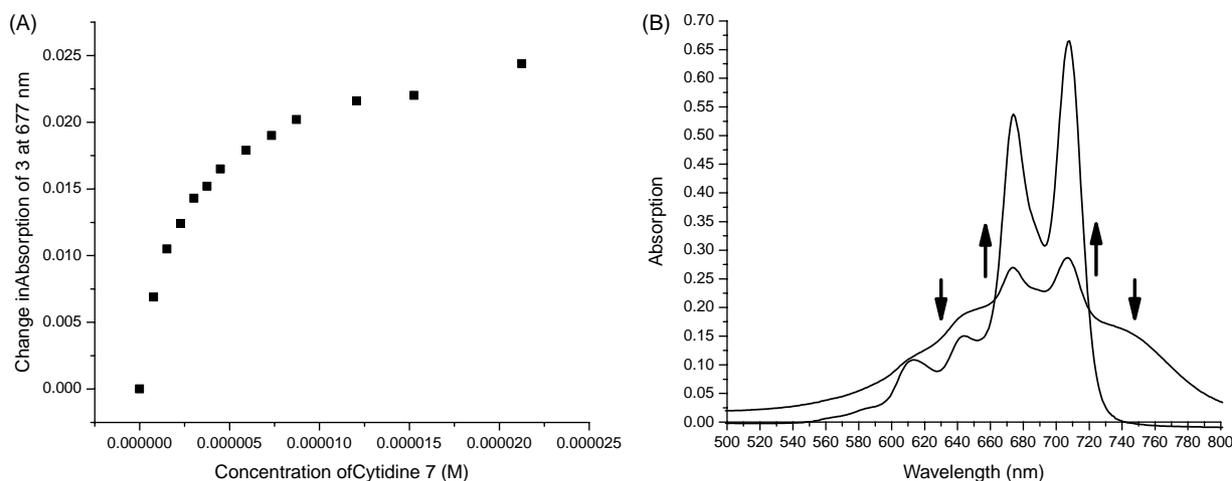

Figure 3. (A) A plot depicting the change in ZnPc **3** (2.5×10^{-6} M) absorption at 677 nm versus increasing concentration of cytidine **7** ($0-2.1 \times 10^{-5}$ M), in 20% DCM/toluene. (B) Change in the absorption spectrum of ZnPc **2** (ca. 2.0×10^{-6} M) in 20% DCM/toluene upon addition of a drop of pyridine.
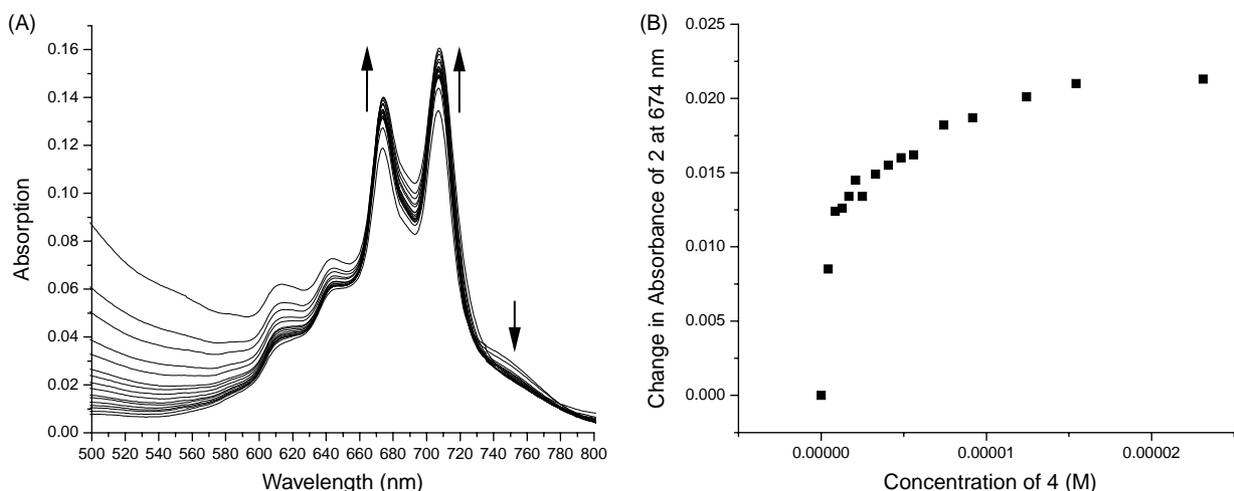
Figure 4. (A) Changes in the absorption spectrum of ZnPc **2** (1.0×10^{-6} M) seen upon the addition of increasing concentrations of **4** (0–2.3×10^{-5} M) in 20% DCM/toluene. (B) Plot showing the change in ZnPc **2** (1.0×10^{-6} M) absorption intensity at 674 nm versus concentration of **4** (0–2.3×10^{-5} M) in 20% DCM/toluene.

Electronic absorption spectroscopy was employed to detect the de-aggregation process caused by the addition of guanosine tethered fullerene **4**. For this experiment, the conditions were chosen such that the monomeric species of **2** as well as the aggregated form are both present in solution (i.e., $[\mathbf{2}] \sim 1.0 \times 10^{-6}$ M in 20% DCM/toluene). The results from this experiment are shown in Figure 4. The Q-band region corresponding to the monomeric species is seen to increase upon increasing concentration of **4** (0–2.3×10^{-5} M). In fact, a plot of absorption at 674 nm (a band that is attributed to the monomeric species) versus concentration of guanosine **4** (see Fig. 4b), results in a sharp increase followed by a plateau. This behavior is interpreted as being caused by an increase in monomer concentration as a result of the addition of increasing aliquots of **4**.

More evidence for de-aggregation came from the observation that the broad shoulder at 750 nm decreases in intensity, albeit by a small amount. Unfortunately, a decrease of the low intensity, blue-shifted, aggregate band, which overlaps the vibrational bands of the monomer was not observed. The reason for this is due to the concomitant increase of a rather high intensity absorption band of **4** in this region of the spectrum.

3.3. De-aggregation experiments with guanosine (5) and C$_{60}$ (6)

Similar de-aggregation experiments were pursued using the guanosine control compound **5** to confirm that the guanosine subunit was capable of base-pairing with the cytidine subunit of **2** and as a consequence, disrupting self-aggregation. The results (Fig. 5) show a clear increase in the monomeric bands at 674 (see Fig. 5b) and 708 nm upon the addition of increasing quantities of guanosine **5** (0–6.9×10^{-5} M). In addition, the region between 600–660 nm shows spectral features characteristic of de-aggregation. In particular, the broad band ascribed to the aggregated species was seen to decrease in intensity, while the vibrational satellites corresponding to the monomeric species became more distinct. The shoulder at 750 nm was also seen to disappear upon adding increasing

concentrations of **5**. These observations, in conjunction with the presence of clean isosbestic points at 662 and 723 nm, are considered as prima facie evidence that the guanosine motif is capable of de-aggregating the ensemble(s) resulting from the self-assembly of the cytidine-linked ZnPc **2**.

UV–vis titrations of ZnPc **2** with C$_{60}$ **6** in 20% DCM/toluene were also carried out in an effort to determine whether the fullerene moiety is also capable of breaking up aggregates formed from ZnPc **2**. As shown in Figure 6, titration of C$_{60}$ **6** (0–2.2×10^{-5} M) into a solution of **2** (1.3×10^{-6} M) gives rise to typical de-aggregation behavior. Here, the absorption corresponding to the monomer increases in intensity (see Fig. 6b), while spectral features corresponding to the aggregate decrease in intensity. These findings, support the notion that fullerene, with electron accepting capabilities, can interact with ZnPc which possesses electron donating features.

These de-aggregation studies lead us to suggest that both guanosine and C$_{60}$ motifs can effect de-aggregation of ZnPc–cytidine conjugate **2**. In addition, the de-aggregation is thought to occur, for the most part, as a result of either base-pairing (in the case of compounds **4** and **5**) or π–π interactions (in the case of **4** and **6**).

3.4. Control studies with ZnPc (3)

While it is not surprising that guanosine derivatives **4** and **5** can disrupt ZnPc–cytidine **2** aggregation as a result of base-pairing, other interactions (such axial ligation of guanosine with the metal center) should also be taken into account. Control experiments, involving ZnPc **3** and the aggregation disruptors **4**, **5** and **6** in 20% DCM/toluene, were undertaken in an effort to gain a further understanding of how these latter species can interact with the macrocycle core. Titrations involving all three guest compounds gave rise to similar observations. Specifically, the absorption maximum at 677 nm is seen to decrease in intensity upon addition of all three guests. A typical spectrum is shown in Figure 7a. Despite the relatively small change in absorbance
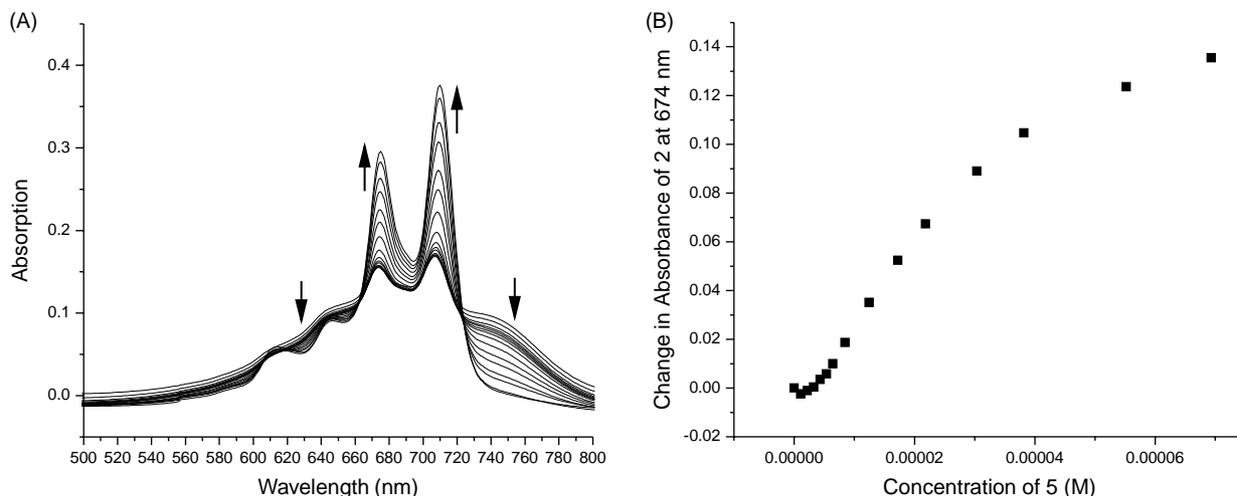
Figure 5. (A) Changes in the absorption spectrum of ZnPc **2** (1.3×10^{-6} M) seen upon the addition of increasing concentrations of guest **5** ($0–6.9 \times 10^{-5}$ M) in 20% DCM/toluene. (B) Plot depicting the change in absorption intensity of **2** (1.3×10^{-6} M) at 674 nm versus concentration of guest **5** ($0–6.9 \times 10^{-5}$ M) in 20% DCM/toluene.

intensity seen over the course of the titration, the structures of the resulting curves (Fig. 7b) suggest that all three guest molecules are involved in binding.[19] These results serve to verify that the C$_{60}$ subunit can interact with the ZnPc core. More interestingly, the results also lead to the inference that the guanosine motif per se also has some affinity for the ZnPc core. One possible mode of interaction of guanosine with ZnPc **3** is through coordination of the N7 nitrogen to the central Zn atom.[16]

3.5. Fluorescence spectroscopy

Fluorescence spectroscopy can also be used as a tool to investigate aggregation in Pc systems, since aggregate formation results in significant quenching of fluorescence.[6,7] Accordingly, the fluorescence emission of ZnPc **2** was monitored as increasing aliquots of disruptor molecules **4**, **5**, and **6**, respectively, in 20% DCM/toluene, were added. As expected, addition of guanosine **5** and C$_{60}$ **6** resulted in an increase in the fluorescence emission followed by saturation

behavior (Fig. 8b). These observations are consistent with the UV–vis studies (see Sections 3.3 and 3.4 supra), and support the proposal that the addition of either **5** or **6** induces de-aggregation of ZnPc **2**.

Interestingly, the maximum increase in fluorescence emission upon the addition of guanosine **5** ($I/I_0 = 2.4$) is significantly larger than the maximum for C$_{60}$ **6** ($I/I_0 = 1.7$). The reason for the lower I/I_0 value is thought to reflect photoinduced electron transfer from the photoexcited ZnPc **2** to C$_{60}$ **6**.[5] In accord with such an explanation, titration of fulleropyrrolidine **4** into a solution of ZnPc **2** (see Fig. 8a), showed almost no increase in fluorescence intensity (maximum value for $I/I_0 \sim 1.0$). Instead, a clear decrease in the intensity of fluorescence emission is observed. While not yet studied in detail, this decrease in intensity is attributed to intra-complex photoinduced electron transfer, which outweighs any increase in fluorescence emission resulting from effecting the de-aggregation of **2**. The nature and time scale of the photoinduced electron transfer process
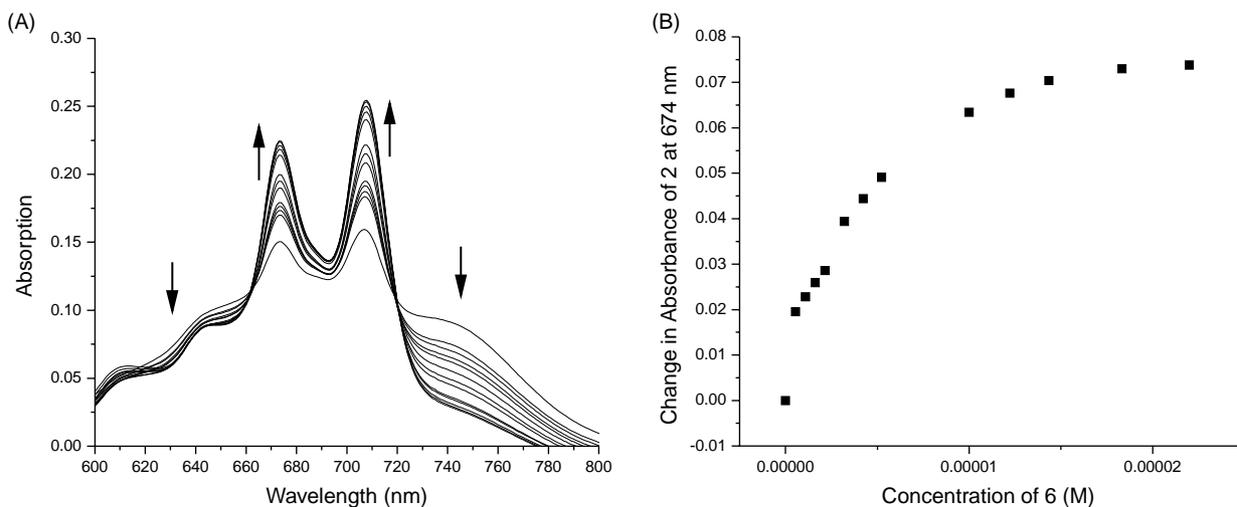

Figure 6. (A) Changes in the absorption spectrum of ZnPc **2** (1.3×10^{-6} M) seen upon the addition of increasing concentrations of guest **6** ($0–2.2 \times 10^{-5}$ M) in 20% DCM/toluene. (B) A plot illustrating the change in ZnPc **2** (1.3×10^{-6} M) absorption at 674 nm versus concentration of **6** ($0–2.2 \times 10^{-5}$ M) in 20% DCM/toluene.
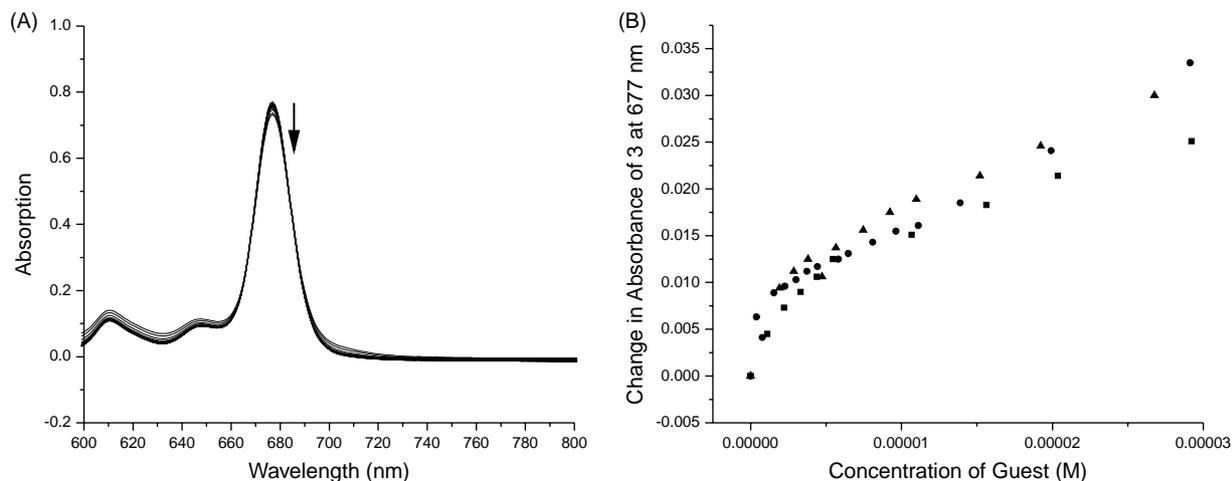
Figure 7. (A) Changes in the absorption spectrum of ZnPc **3** (2.5×10^{-6} M) seen upon the addition of increasing concentrations of **4** ($0–2.9 \times 10^{-5}$ M) in 20% DCM/toluene. (B) Plot depicting the change in ZnPc **3** ($\sim 3.0 \times 10^{-6}$ M) absorption intensity at 677 nm versus concentration of guest (**4** (●), **5** (■), and **6** (▲)) in 20% DCM/toluene.

between ZnPc–cytidine **2** and fullerene tethered guanosine **4** is currently being investigated in our laboratories. Results from these studies will be published in due course.

4. Conclusion

Taken in concert the above results indicate that the cytidine–ZnPc hybrid **2** is highly 'narcissistic'; as it undergoes self-assembly even at low concentrations in 20% DCM/toluene as a result of using both π–π interactions and cytidine macrocycle interactions. The resulting aggregate(s) can be broken up by the addition of guanosine, a nucleic acid base that can serve to tie up the cytidine functionality through base-pairing interactions. Additionally, guanosine can also directly interact with the metal center of the macrocycle. An alternative method of de-stabilizing the aggregate is to use the fullerene motif. This motif can compete with macro-cycle–macrocycle π–π stacking interactions. The results of this paper thus serve to illustrate that fullerene and

guanosine, icon-like entities in supramolecular chemistry, can be used to modulate phthalocyanine aggregation.

5. Experimental

5.1. General

Melting points were determined using a Buchi melting point apparatus and are uncorrected. ^{1}H NMR spectra were obtained on a Bruker AC-300 (300 MHz) spectrometer. Mass-spectra were determined on a VG AustoSpec apparatus. Elemental analyses were performed on a Perkin-Elmer 2400 CHN elemental analyzer. UV–vis spectra were taken on a Beckman DU 540 spectropho-tometer. Fluorescence measurements were obtained using a SPEX-332 spectrofluorimeter. Fluorescence titrations were carried out by exciting the samples at the isosbestic points, where possible. Otherwise, the fluorescence emission was corrected for variations in the absorptions. The solvents
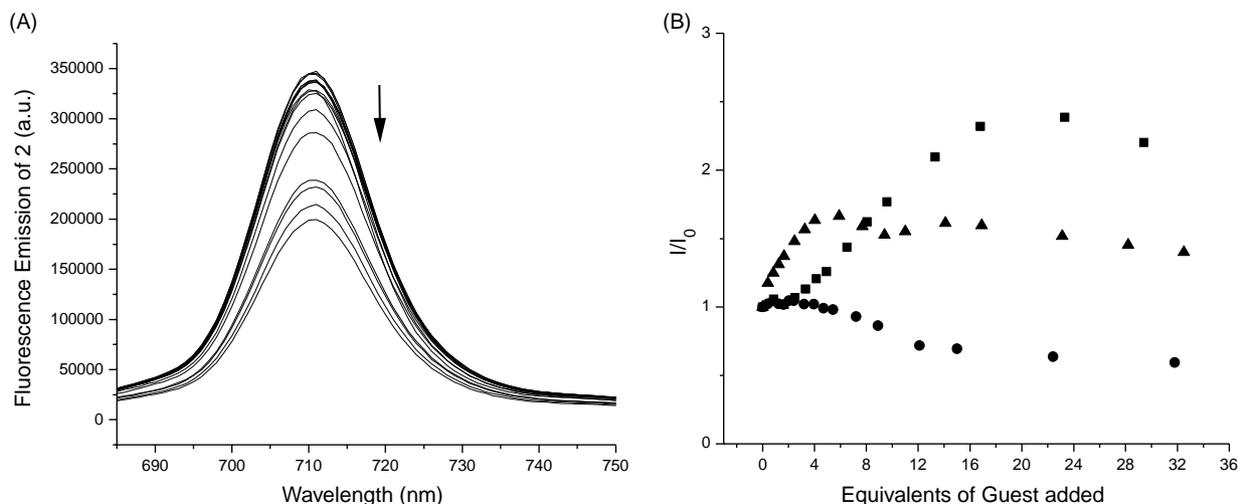

Figure 8. (A) Changes in the emission spectrum of **2** (1.0×10^{-6} M) seen upon the addition of **4** ($0–3.3 \times 10^{-5}$ M) in 20% DCM/toluene; excitation wavelength 660 nm. (B) Plot of the change in fluorescence intensity of **2** as a ratio of I/I_0 versus equivalents of guest (**4** (●), **5** (■), and **6** (▲)) in 20% DCM/toluene. For titration of **2** with **4**: (excitation at 660 nm), [**2**]$=1.0 \times 10^{-6}$ M and [**4**]$=0–3.3 \times 10^{-5}$ M. For titration of **2** with **5**: (excitation at 662 nm), [**2**]$=1.3 \times 10^{-6}$ M and [**5**]$=0–3.8 \times 10^{-5}$ M. For titration of **2** with **6**: (excitation at 662 nm), [**2**]$=1.3 \times 10^{-6}$ M and [**6**]$=0–4.2 \times 10^{-5}$ M.

used for spectroscopic analyses were ACS spectranalyzed DCM (Fischer) and spectrophotometric grade toluene (ACROS).

Control **3** was prepared using a standard procedure.[20] Fullerene **6** was used as purchased from MER corporation. Nucleobases **5** and **7** were synthesized using standard protection protocols.[21] Synthetic compound **4** was prepared as described elsewhere.[17]

5.1.1. 4-Amino-5-[5″-ethynyl-tri-*tert*-butylphthalocyani-natoZn(II)]-1-[2′,3′,5′-tri-*O*-(*tert*-butyl-dimethylsilyl)-β-ᴅ-ribofuranosidyl]-pyrimidin-2-one (2).

To a mixture of tri-*tert*-butyl(ethynyl)phthalocyaninatozinc[22] (77 mg, 0.1 mmol) and iodocytidine[23] (86 mg, 0.12 mmol) in dry toluene (10 ml) and triethylamine (1 ml) under argon atmosphere, CuI (2 mg, 10 μmol) and Pd(PPh₃)₄ (11.5 mg, 10 μmol) were added. The reaction mixture was then stirred and heated at 50 °C overnight. After cooling, the solvents were removed in vacuo and the crude product was purified by flash column chromatography (SiO₂, methanol/dichloromethane 1:100), yielding **2** as a green solid (75 mg, 55%): mp >250 °C (decomp.); UV–vis (CH₂Cl₂) λ_{max} (nm) (log ε): 679 (5.12), 347 (5.03); ¹H NMR (300 MHz, CD₂Cl₂ with a drop of CD₃OD) δ 8.9–7.2 (br×m, 12H), 5.9–5.7 (m, 1H), 4.3–4.0 (m 4H), 3.8 (m 1H), 1.9–1.5 (m, 27H), 1.07 (s, 9H), 0.95 (s, 9H), 0.93 (s, 9H), 0.32 (s, 6H), 0.17 (s, 3H), 0.14 (s, 3H), 0.13 (s, 3H), 0.09 (s, 3H); ¹³C NMR (75 MHz, CD₂Cl₂ with a drop of CD₃OD) δ 163.2, 153.5, 148.9, 143.2, 142.5, 138.5, 133.8, 133.4, 131.00, 128.9, 126.6, 125.7, 120.3, 118.7, 95.0, 90.7, 89.0, 83.9, 80.3, 76.0, 70.0, 61.8, 36.1, 32.3, 29.1, 25.6, 24.8, 17.8, 17.5, 17.2, −5.2, −5.5, −5.9; ESI-MS: *m/z* 1354–1358 [M]⁺: calcd for **2** C₇₃H₉₃N₁₁O₅Si₃Zn: C 64.74, H 6.92, N 11.38; found C 64.32, H 6.83, N 11.06.

References and notes

 1. (a) Kadish, K. M., Smith, K. M., Guillard, R., Eds.; *The Porphyrin Handbook*; Academic: San Diego, 2003; Vols. 15–20. (b) Leznoff, C. C., Lever, A. B. P., Eds.; *Phthalocyanines: Properties and Applications*; VCH: Weinheim, 1989, 1993, 1996; Vols. 1–4. (c) Hanack, M.; Heckmann, H.; Polley, R. In Schaumann, E., Ed.; *Methods in Organic Chemistry*; Thieme: Stuttgart, 1998; Vol. E9d, p 717. (d) de la Torre, G.; Nicolau, M.; Torres, T. In *Phthalocyanines: Synthesis, Supramolecular Organization and Physical Properties*; Nalwa, H. S., Ed.; Academic: New York, 2001.

 2. (a) Fabian, J.; Nakazumi, H.; Matsuoka, M. *Chem. Rev.* **1992**, *92*, 1197. (b) Schmidt, H.-W. *Adv. Mater.* **1989**, *1*, 218. (c) Birkett, D. *Chem. Ind.* **2000**, *5*, 178. (d) Kuder, J. E. *J. Imaging Sci.* **1988**, *32*, 51.

 3. (a) de la Torre, G.; Vázquez, P.; Agulló-López, F.; Torres, T. *J. Mater. Chem.* **1998**, *8*, 1671. (b) de la Torre, G.; Vázquez, P.; Agulló-Lopéz, F.; Torres, T. *Chem. Rev.* **2004**, *104*, 3723.

 4. (a) Bonnett, R. *Chem. Soc. Rev.* **1995**, *24*, 19. (b) Xue, L. Y.; Chiu, S. M.; Oleinick, N. L. *Oncogene* **2001**, *20*, 3420.

 5. (a) Linssen, T. G.; Durr, K.; Hanack, M.; Hirsch, A. *J. Chem. Soc., Chem. Commun.* **1995**, 103. (b) El-Khouly, M. E.; Ito, O.; Smith, P. M.; D'Souza, F. *J. Photochem. Photobiol., C* **2004**, *5*, 79. (c) Nojiri, T.; Alam, M. M.; Konami, H.; Watanabe, A.; Ito, O. *J. Phys. Chem. A* **1997**, *101*, 7943. (d) Guldi, D. M.; Gouloumis, A.; Vázquez, P.; Torres, T. *Chem. Commun.* **2002**, 2056. (e) Guldi, D. M.; Zilbermann, I.; Gouloumis, A.; Vázquez, P.; Torres, T. *J. Phys. Chem. B* **2004**, *108*, 18485. (f) Loi, M. A.; Denk, P.; Hoppe, H.; Neugebauer, H.; Winder, C.; Meissner, D.; Brabec, C. J.; Sariciftci, N. S.; Gouloumis, A.; Vázquez, P.; Torres, T. *J. Mater. Chem.* **2003**, *13*, 700.

 6. Snow, A. W. In Kadish, K. M., Smith, K. M., Guillard, R., Eds.; The Porphyrin Handbook; Academic: San Diego, 2003; Vol. 17, p 129.

 7. George, R. D.; Snow, A. W.; Shirk, J. S.; Barger, W. R. *J. Porphyrins Phthalocyanines* **1988**, *2*, 1.

 8. (a) Martin, P. C.; Gouterman, M.; Pepich, B. V.; Renzoni, G. E.; Schindele, D. C. *Inorg. Chem.* **1991**, *30*, 3305. (b) Dhami, S.; de Mello, A. J.; Rumbles, G.; Bishop, S. M.; Phillips, D.; Beeby, A. *Photochem. Photobiol.* **1995**, *61*, 341.

 9. (a) Cook, M. J.; Chambrier, I. In Kadish, K. M., Smith, K. M., Guillard, R., Eds.; The Porphyrin Handbook; Academic: San Diego, 2003; Vol. 17, p 37. (b) Law, K.-Y. *Chem. Rev.* **1993**, *93*, 449.

10. (a) See Ref. 6 (b) Schutte, W. J.; Sluyters-Rehbach, M.; Sluyters, J. H. *J. Phys. Chem.* **1993**, *97*, 6069. (c) Fujiki, M.; Tabei, H.; Kurihara, T. *J. Phys. Chem.* **1988**, *92*, 1281. (d) de la Escosura, A.; Martínez-Díaz, V. M.; Thordarson, P.; Rowan, A. E.; Nolte, R. J. M.; Torres, T. *J. Am. Chem. Soc.* **2003**, *125*, 12300. (e) Engel, M. K.; Bassoul, P.; Bosio, L.; Lehmann, H.; Hanack, M.; Simon, J. *Liq. Cryst.* **1993**, *15*, 709. (f) Li, X.-Y.; Ng, D. K. P. *Tetrahedron Lett.* **2001**, 305.

11. (a) Martínez-Díaz, V. M.; Fender, N. S.; Rodríguez-Morgade, S. M.; Gómez-López, M.; Diederich, F.; Echegoyen, L.; Stoddart, F. J.; Torres, T. J. *Mater. Chem.* **2002**, *12*, 2095. (b) Guldi, D. M.; Ramey, J.; Martínez-Díaz, V. M.; de la Escosura, A.; Torres, T.; Da Ros, T.; Prato, M. *Chem. Commun.* **2002**, 2774. (c) Guldi, D. M.; Gouloumis, A.; Vázquez, P.; Torres, T.; Georgakilas, V.; Prato, M. *J. Am. Chem. Soc.* **2005**, *127*, 5811.

12. For a review on synthetic ensembles prepared through base-pairing interactions see: Sessler, J. L.; Jayawickramarajah, J. *Chem. Commun.* **2005**, 1939.

13. Increasing the rigidity of the linkers in nucleobase derived systems can dramatically enhance association through base-pairing interactions. See: Sessler, J. L.; Wang, B.; Harriman, A. *J. Am. Chem. Soc.* **1993**, *115*, 10418.

14. Lee, L. K.; Sabellli, N. H.; LeBreton, P. R. *J. Phys. Chem.* **1982**, *86*, 3926.

15. The split Q-band is attributed to the monomeric species and not to aggregation. This is because when pyridine (a ligand

that can coordinate to the Zn metal center and thereby effect de-aggregation) is added to the solution, the split Q-band persists. In contrast, the aggregation bands (centered at 630 and 750 nm, respectively) completely disappear.

16. For examples of nucleobases coordinating through axial ligation to metal centers within a macrocyclic framework see: (a) Ogoshi, H.; Hatakeyama, H.; Yamamura, K.; Kuroda, Y. *Chem. Lett.* **1990**, 51. (b) Ogoshi, H.; Hatakeyama, H.; Kotani, J.; Kawashima, A.; Kuroda, Y. *J. Am. Chem. Soc.* **1991**, *113*, 8181.

17. Sessler, J. L.; Jayawickramarajah, J.; Gouloumis, A.; Torres, T.; Guldi, D. M.; Maldonado, S.; Stevenson, K. J. *Chem. Commun.* **2005**, 1892.

18. (a) Satake, A.; Kobuke, Y. *Tetrahedron* **2005**, *61*, 13 and references therein. (b) Boyd, P. D. W.; Hodgson, M. C.; Rickard, C. E. F.; Oliver, A. G.; Chaker, L.; Brothers, P. J.; Bolskar, R. D.; Tham, F. S.; Reed, C. A. *J. Am. Chem. Soc.* **1999**, *121*, 10487. (c) Mizuseki, H.; Igarashi, N.; Belosludov, R. V.; Farajian, A. A.; Kawazoe, Y. *Synth. Met.* **2003**, *138*, 281. (d) El-Khouly, M. E.; Islam, S. D.-M.; Fujitsuka, M.; Ito, O. *J. Porphyrins Phthalocyanines* **2000**, *4*, 713. (e) Kessler, B. *Appl. Phys. A* **1998**, *67*, 125.

19. To confirm that compounds **4**, **5**, and **6** were indeed binding with control **3**, fluorescence emission of **3** was monitored (excitation at 656 nm) as a function of increasing concentrations of **4**, **5**, and **6**, respectively. Addition of all three compounds resulted in a decrease in fluorescence (monitored at 684 nm), substantiating the notion that they can interact with ZnPc **3**.

20. Mosers, F. M.; Thomas, A. L. In *Phthalocyanines*, *Vol. 2*; CRC: Boca Raton, Fl, 1983; Chapter 1.

21. Hayakawa, H.; Haraguchi, K.; Tanaka, H.; Miyasaka, T. *Chem. Pharm. Bull.* **1987**, *35*, 72.

22. Maya, E. M.; Vázquez, P.; Torres, T. *Chem. Eur. J.* **1999**, *5*, 2004.

23. Sessler, J. L.; Brown, C. T.; Wang, R.; Hirose, T. *Inorg. Chim. Acta* **1996**, *251*, 135.